High Energy Gain of Trapped Electrons in a Tapered, Diffraction-Dominated Inverse-Free-Electron Laser

P. Musumeci,[1] S. Ya. Tochitsky,[2] S. Boucher,[1] C. E. Clayton,[2] A. Doyuran,[1] R. J. England,[1] C. Joshi,[2] C. Pellegrini,[1] J. E. Ralph,[2] J. B. Rosenzweig,[1] C. Sung,[2] S. Tolmachev,[3] G. Travish,[1] A. A. Varfolomeev,[3] A. A. Varfolomeev, Jr.,[3] T. Yarovoi,[3] and R. B. Yoder[1]

[1]*Neptune Laboratory, Department of Physics and Astronomy, UCLA, Los Angeles, California 90095, USA*
[2]*Department of Electrical Engineering, UCLA, Los Angeles, California 90095, USA*
[3]*Russian Research Centre Kurchatov Institute, Moscow 123182, Russia*

(Received 18 October 2004; published 20 April 2005)

Energy gain of trapped electrons in excess of 20 MeV has been demonstrated in an inverse-free-electron-laser (IFEL) accelerator experiment. A 14.5 MeV electron beam is copropagated with a 400 GW CO_2 laser beam in a 50 cm long undulator strongly tapered in period and field amplitude. The Rayleigh range of the laser, $\sim$1.8 cm, is much shorter than the undulator length yielding a diffraction-dominated interaction. Experimental results on the dependence of the acceleration on injection energy, laser focus position, and laser power are discussed. Simulations, in good agreement with the experimental data, show that most of the energy gain occurs in the first half of the undulator at a gradient of 70 MeV/m and that the structure in the measured energy spectrum arises because of higher harmonic IFEL interaction in the second half of the undulator.

DOI: 10.1103/PhysRevLett.94.154801 PACS numbers: 41.60.Cr, 41.75.Jv, 41.75.Lx

The inverse-free-electron-laser (IFEL) mechanism to accelerate particles has been proposed as an advanced acceleration scheme for many years [1,2]. In an IFEL, relativistic particles copropagate with a laser beam through an undulator magnet. The undulator produces a small transverse velocity (wiggling motion) in a direction parallel to the electric vector of the electromagnetic wave so that energy can be transferred from the wave to the particles. Efficient energy exchange takes place when the electron phase slippage in the wave is such that its transverse velocity changes sign synchronously with the laser field (resonant condition [3]).

Successful proof-of-principle IFEL experiments have shown that, along with acceleration [4,5], this scheme offers the possibility of manipulating and controlling the longitudinal phase space of the electron beam on the laser wavelength scale. First among other laser accelerator schemes [6], the IFEL has experimentally demonstrated beam microbunching at the laser wavelength [7], phase-dependent acceleration [8], phase-locked external injection using a buncher-accelerator scheme [9], and high trapping efficiency and control of final energy spread [10]. Despite this significant progress, in all these experiments the energy gain was modest and the measured acceleration gradient was well below that achieved in conventional rf accelerators ($\sim$50 MeV/m).

It is of great importance to demonstrate both high energy gain and acceleration gradient in a laser accelerator. This can be achieved not only by increasing the coupled laser power, but also by increasing the effective interaction length. The latter is obtained (i) by extending the region where the laser is most intense (diffraction effects) and (ii) by increasing the length over which the particles and the laser wave maintain synchronism (tapering).

In this Letter, we demonstrate both 150% (20 MeV) energy gain and 70 MeV/m accelerating gradient obtained in the IFEL experiment at the Neptune Laboratory at UCLA. These high energy gain and high gradient results were achieved by employing a 400 GW CO_2 laser beam with a focal intensity of 2×10^{14} W/cm^2 (about 2 orders of magnitude more than in any previous IFEL experiment [9,10]) in a 50 cm long undulator strongly tapered in period and magnetic field amplitude. Approximately 5% of injected electrons were self-trapped (microbunched) within the IFEL ponderomotive potential well. We also report for the first time the second harmonic IFEL interaction manifested in the observed modulation of the output electron energy spectrum.

A schematic of the experimental layout is shown in Fig. 1. A 14.5 MeV energy electron beam with a charge of 300 pC, a normalized emittance of 5 mm mrad, and a rms pulse length of 6 ps was injected in the IFEL undulator [11] using the Neptune rf photoinjector [12]. Final focus quadrupoles focused the e beam to the spot size of 120 μm (rms) in the middle of the undulator. The 10.6 μm CO_2 laser beam [13] was focused to a spot size ($1/e^2$) of 240 μm using a 2.56 m focal length NaCl lens which

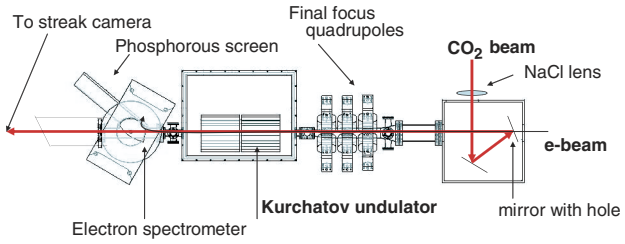

FIG. 1 (color online). Layout of the Neptune IFEL experiment.

also served as a vacuum window. The laser beam was made collinear to the e beam utilizing a plane copper mirror with a hole located 1.45 m upstream of the magnet entrance. The beams were aligned on a probe in the middle of the undulator with an accuracy of 100 μm in offset and 1 mrad in angle. After the interaction region, the e beam was energy analyzed by a Browne-Buechner wide bandwidth magnetic spectrometer. The laser beam exiting the undulator was sent to the streak camera for timing measurements.

The IFEL hybrid planar undulator KIAE-2p [11] was designed and built at the Kurchatov Institute. This magnet was optimized for a 400 GW, 3.6 cm Rayleigh range driver laser beam. It has a very strong variation of the wiggling period and magnetic field amplitude along the axis (see Table I), carefully tailored to maintain the resonance condition of the IFEL interaction between the CO_2 photons and the quickly accelerating electrons. Because the Rayleigh range is much shorter than the undulator length, the driving field along the undulator varies rapidly, and it becomes important to properly consider the Guoy phase shift experienced by the laser near the focal point [14]. In order to maintain synchronism through the focal region, two undulator sections were built with the field in the central region adjusted using a corrector Vanadium-Permandur plate. The undulator period and field strength were specified using simulation results [11] obtained with the three-dimensional code TREDI [14].

Synchronization between electron and laser pulses is critical for every laser accelerator with an externally injected electron beam. To maximize the acceleration, the 15 ps FWHM electron bunch must be synchronized with the peak of the 240 ps FWHM laser pulse. In order to get very accurate information on the relative timing between the electrons and the amplified CO_2 pulse on each shot, we set up a streak-camera-based diagnostic. The cathode of the streak camera is not sensitive to 10.6 μm photons, so an optical gating technique, based on the Kerr effect, was used to gate a long red laser diode with the CO_2 pulse. This gated portion of red pulse is sent on the entrance slit of a 10 ps resolution streak camera together with a small fraction of the photocathode driver laser as reference for the electron-beam timing. In Fig. 2, the final maximum energy of the IFEL accelerator is shown as a function of delay between the e-beam reference pulse and the peak of the CO_2 pulse, as measured on the streak camera. A lineout of a typical CO_2 pulse is also displayed on the same time scale. Even for very small laser power, some interaction is observed (+150 ps data). On the other hand, the output energy is clearly maximized when the electrons sample the peak laser intensity. The relatively low energy gain shown in this set of data is due, as we will explain later, to the fact that this measurement was performed with the laser focused at the undulator midpoint. Note that the high power laser system has an intrinsic jitter in laser power as large as $\pm 50\%$ which results in fluctuations in the time of arrival of ± 50 ps [15]. This diagnostic allowed us to determine for each laser shot the pulse length—and thus the peak power—of the CO_2 beam and which part of the laser pulse intensity profile the electron beam sampled with an accuracy of ± 10 ps. This measurement was used to optimize the injection time of the electrons in the IFEL accelerator.

TABLE I. Parameters of the 50 cm long undulator.

	Initial	Final
Undulator period	1.5 cm	5 cm
Magnetic field amplitude	0.116 T	0.686 T
Normalized undulator K	0.2	2.8
Resonant energy	14.5 MeV	52 MeV
Gap	12 mm	12 mm

The optical scheme used in the experiment to focus and control the transverse size of the laser beam size is also very important. To remain below the damage threshold of 2 J/cm^2 on the last turning mirror (see Fig. 1), we operated with a focal spot size of 240 μm corresponding to a Rayleigh range of 1.8 cm, about half of the original design value. This stronger focusing leads to a larger variation of the laser beam size along the interaction region and, for a focus position at the undulator midpoint, to a larger and less intense beam at the magnet entrance and exit. This leads to a degradation of the IFEL accelerator performance, i.e., the number of trapped particles and the final maximum electron energy. Moreover, the laser-electron-beam alignment becomes more critical because of the smaller laser spot size.

The reduction in the IFEL performance can be minimized, however, by moving the laser focus upstream from the undulator midpoint, which increases the intensity at the magnet entrance above the trapping threshold and allows the acceleration process to correctly proceed early in the undulator. In Fig. 3, we show the output energy of the IFEL accelerator versus the laser focus position. Also shown are the intensity of a 400 GW, 1.8 cm Rayleigh range laser beam (solid line) and the trapping threshold intensity (dashed line), both calculated at the entrance plane of the magnet. Positioning the laser focus 2 cm ($\sim$1 Rayleigh range) upstream of the undulator midpoint was found to give the maximum final energy. When moving the focus towards the undulator center, the intensity at the magnet

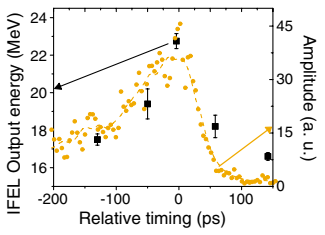

FIG. 2 (color online). IFEL output energy versus measured delay on the streak camera between the reference e-beam pulse and the CO_2 laser. Also shown is a typical streak of the CO_2 laser pulse.

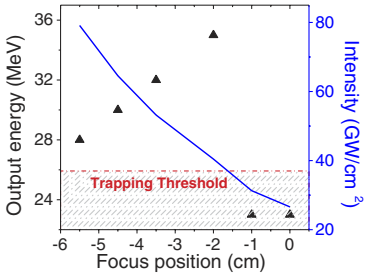

FIG. 3 (color online). IFEL output energy versus laser focus position. As the laser focus is moved towards the undulator center, the laser intensity at the magnet entrance drops below the trapping threshold.

entrance drops below the trapping threshold and there is no resonant IFEL interaction. If the laser focus is moved further upstream from the optimum point, the final energy decreases because the effective interaction length is shortened, due to the electrons falling off the resonance curve earlier in the undulator.

The main diagnostic on the output electron beam was the single-shot spectrum image of the fluorescent phosphor screen located on the exit slit of the wide band energy spectrometer. A typical reconstructed single-shot energy spectrum is shown in Fig. 4. The measured power in the CO_2 pulse for this IFEL shot was 400 GW, and the laser was focused upstream of the nominal position by 2 cm. The accelerator performance has been characterized in terms of the output energy and the fraction of particles above 25 MeV (trapped particles). More than 5% of particles are trapped and accelerated up to 35 MeV (150% energy gain).

The dependencies of the final output energy and fraction of trapped particles on the input e-beam energy Fig. 5(a)] and the laser power [Fig. 5(b)] were also studied. In order to have a better control of the experimental parameters, for these measurements the laser focus was moved 3.5 cm upstream of the undulator center where the trapping threshold was lower (about 300 GW) and the results were more reproducible, because the high power laser system could operate in a more stable regime. The experimental data indicate that the fraction of captured particles [circles in Figs. 5(a) and 5(b)] is more sensitive to variation of the input parameters than the final beam energy [triangles in Figs. 5(a) and 5(b)]. In other words, once the resonant IFEL condition (>14.2 MeV) is reached and the trapping threshold (150 GW) is exceeded, the output energy remains relatively constant. Thereafter, further increase of the injection energy and/or laser power leads to a monotonic increase in the fraction of trapped particles as is apparent in Figs. 5(a) and 5(b).

The input beam has a small energy spread (0.5%) and can be considered monoenergetic for the IFEL interaction. Changing the input electron-beam energy for a fixed laser power corresponds to probing the height of the accelerating bucket in the longitudinal IFEL phase space at the entrance of the undulator. The acceptance energy width can be estimated as the HWHM (~0.4 MeV) of the particle trapping data [circles in Fig. 5(a)], a value that agrees with the one predicted by the theory using the measured undulator and laser parameters [3]. In the same way, increasing (decreasing) the laser power [see Fig. 5(b)] has the effect of expanding (shrinking) the acceptance phase window at the undulator entrance and so of trapping more (less) particles.

When using the experimental parameters, the simulations performed with TREDI agree well with the measured dependencies [lines in Figs. 5(a) and 5(b)]. The simulations also reproduce well the experimental output energy spectrum (solid line in Fig. 4). The differences in the low energy side of the energy spectrum may be due to spatial misalignment and/or laser phase front distortions.

Following the evolution of the maximum-energy particle in these simulations, we obtain the solid red curve shown in Fig. 6(a). The IFEL acceleration mostly takes place in the first 25 cm. Thus an average accelerating gradient of ~70 MeV/m for the undulator first half is deduced, a value comparable to the gradient in state-of-the-art rf structures. A few centimeters after the undulator center, the particles fall off the resonance curve ($n = 1$ line) because the driving laser intensity decreases below the trapping threshold and the acceleration process stops. The detrapping process is increased by the fact that since the laser focus is shifted upstream of the undulator midpoint the Guoy phase shift is not compensated by the appositely designed magnetic correction.

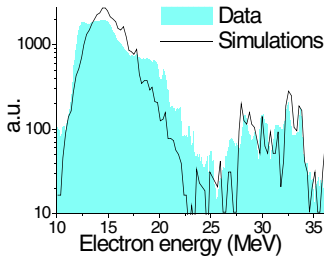

FIG. 4 (color online). Single-shot energy spectrum. The simulated spectrum is normalized to the same area as the measured one.

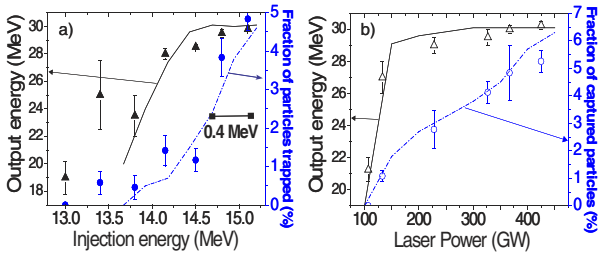

FIG. 5 (color online). IFEL output energy and fraction of trapped particles versus input e-beam energy for 300 GW input laser power (a) and versus driving laser power for 14.5 MeV input energy (b). The lines represent TREDI simulation results.

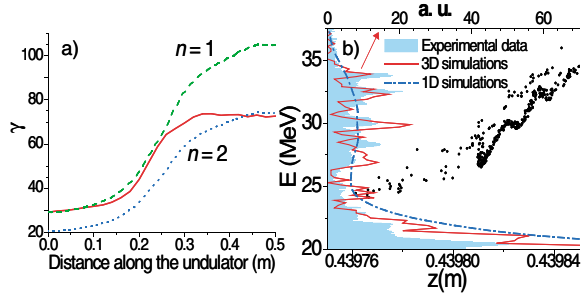

FIG. 6 (color). Simulations of the IFEL experiment. (a) Maximum-energy particle evolution along the undulator. The first and second harmonic resonant curved are also shown. (b) Longitudinal phase space at 45 cm with the energy modulation due to the second harmonic interaction.

Figure 6(b) shows the simulated longitudinal phase space at 45 cm along the undulator (the black dots represent the simulation macroparticles). The solid red line on the left of the graph is the projection of the phase space on the energy axis. Also shown is the measured experimental output spectrum (cyan histogram). The energy modulation appearing in both the simulated and experimental energy spectra is particularly interesting because the spectrum predicted by the solution of the 1D FEL-like equations does not show any peaks (blue dotted line). The high energy side of the 3D simulation spectrum, a few centimeters after the midpoint, develops a peaked structure similar to that observed in the data. Experimentally, this structure was reproducible shot to shot, ruling out the possibility of being caused by microstructures present in the e beam or in the laser beam.

The IFEL resonance condition is ordinarily understood to mean that efficient energy exchange between the transverse electromagnetic wave and the electrons can take place only at electron energies such that, in the electron rest frame, the wiggling induced by the laser has the same frequency as the wiggling induced by the undulator. However, when the motion in the electron rest frame is not a simple dipole oscillation (e.g., for undulator $K \geq 1$), resonance can also occur if laser frequency is a *multiple* of the undulator wiggling frequency; that is, electrons of a fixed energy may interact not only with the fundamental radiation frequency but also with its harmonics [16]. From another point of view, particles of different energies $\gamma_{r,n}$ can interact with the same laser frequency, because they see the electromagnetic wave as a higher harmonic of the fundamental frequency with which they are resonant. In other words, for a given laser wavelength and undulator magnet, there are multiple resonant energies $\gamma_{r,n} = [\lambda_w(1 + K^2/2)/2n\lambda]^{1/2}$. As discussed earlier, in the Neptune IFEL experiment the electrons fall off the resonant curve soon after the midpoint [see Fig. 6(a)]. A few centimeters later, their energy is a factor of $\sqrt{2}$ less than the first harmonic resonant energy ($n = 1$ curve) at that point of the undulator, and therefore the electrons are resonant with the $n = 2$ curve and can exchange energy with the 10.6 μm photons via the second harmonic IFEL interaction. Although even harmonic coupling is suppressed in a planar perfectly collinear geometry, the large angles inherent of our diffraction-dominated IFEL scheme imply a finite second harmonic coupling [17]. We believe this is the origin of the final output energy modulation seen in both experiment and simulation [Fig. 6(b)]. The higher (even and odd) harmonic IFEL interaction adds a degree of freedom (the harmonic coupling number n) in the design of magnetic systems capable of coupling lasers and electron beams and constitutes a possible alternative to the resonant coupling when, for a given electron-beam energy and laser wavelength, the parameters of the required IFEL undulator are unfeasible.

In conclusion, in the Neptune Laboratory IFEL experiment, we studied the interaction of relativistic electrons and a diffracting high power laser beam in a strongly tapered undulator. We observed an energy gain larger than 20 MeV (>150% relative energy gain) and an energy gradient of ~70 MeV/m. The energy gain is the highest obtained to date with an IFEL accelerator. Self-trapping of particles in a stable accelerating bucket from an initial unmicrobunched distribution was also demonstrated. Finally, higher harmonic IFEL interaction was observed in the second section of the undulator.

This work is supported by U.S. Department of Energy Grants No. DE-FG03-92ER40693 and No. DE-FG03-92ER40727.

[1] R. Palmer, IEEE Trans. Nucl. Sci. **28**, 3370 (1981).
[2] E. D. Courant, C. Pellegrini, and W. Zakowicz, Phys. Rev. A **32**, 2813 (1985).
[3] N. M. Kroll, P. L. Morton, and M. N. Rosenbluth, IEEE J. Quantum Electron. **17**, 1436 (1981).
[4] I. Wernick and T. C. Marshall, Phys. Rev. A **46**, 3566 (1992).
[5] A. Van Steenbergen *et al.*, Phys. Rev. Lett. **77**, 2690 (1996).
[6] *Laser Acceleration of Particles*, edited by P. J. Channel, AIP Conf. Proc. No. 91 (AIP, New York, 1982).
[7] Y. Liu *et al.*, Phys. Rev. Lett. **80**, 4418 (1998).
[8] R. B. Yoder, T. C. Marshall, and J. L. Hirshfield, Phys. Rev. Lett. **86**, 1765 (2001).
[9] W. Kimura *et al.*, Phys. Rev. Lett. **86**, 4041 (2001).
[10] W. Kimura *et al.*, Phys. Rev. Lett. **92**, 054801 (2004).
[11] A. A. Varfolomeev *et al.*, Nucl. Instrum. Methods Phys. Res., Sect. A **483**, 377 (2002).
[12] S. G. Anderson *et al.*, AIP Conf. Proc. **569**, 487 (2001).
[13] S. Y. Tochitsky *et al.*, Opt. Lett. **24**, 1717 (1999).
[14] P. Musumeci *et al.*, AIP Conf. Proc. **647**, 278 (2002).
[15] S. Y. Tochitsky *et al.*, Phys. Plasmas **11**, 2875 (2004).
[16] Z. Huang and K. J. Kim, Phys. Rev. E **62**, 7295 (2000).
[17] P. Musumeci *et al.* (to be published).